

Citation for published version:

Zarmpi, P, Flanagan, T, Meehan, E, Mann, J & Fotaki, N 2020, 'Surface dissolution UV imaging for characterization of superdisintegrants and their impact on drug dissolution', *International Journal of Pharmaceutics*, vol. 577, 119080. <https://doi.org/10.1016/j.ijpharm.2020.119080>

DOI:

[10.1016/j.ijpharm.2020.119080](https://doi.org/10.1016/j.ijpharm.2020.119080)

Publication date:

2020

Document Version

Peer reviewed version

[Link to publication](#)

Publisher Rights

CC BY-NC-ND

University of Bath

Alternative formats

If you require this document in an alternative format, please contact:
openaccess@bath.ac.uk

General rights

Copyright and moral rights for the publications made accessible in the public portal are retained by the authors and/or other copyright owners and it is a condition of accessing publications that users recognise and abide by the legal requirements associated with these rights.

Take down policy

If you believe that this document breaches copyright please contact us providing details, and we will remove access to the work immediately and investigate your claim.

Surface dissolution UV Imaging for characterization of superdisintegrants and their impact on drug dissolution

P. Zarnpi¹, T. Flanagan^{2,3}, E. Meehan², J. Mann², N. Fotaki^{1,*}

¹Department of Pharmacy and Pharmacology, University of Bath, Bath, United Kingdom

²Pharmaceutical Technology & Development, AstraZeneca, Macclesfield, UK

³Currently at UCB Pharma, Chemin du Foriest, B – 1420 Braine-l’Alleud, Belgium

* Corresponding Author

Dr Nikoletta Fotaki

Department of Pharmacy and Pharmacology

University of Bath, Claverton Down

Bath, BA2 7AY

United Kingdom

Tel. +44 1225 386728

Fax: +44 1225 386114

E-mail: n.fotaki@bath.ac.uk

Abstract

Superdisintegrants are a key excipient used in immediate release formulations to promote fast tablet disintegration, therefore understanding the impact of superdisintegrant variability on product performance is important. The current study examined the impact of superdisintegrant critical material attributes (viscosity for sodium starch glycolate (SSG), particle size distribution (PSD) for croscarmellose sodium (CCS)) on their performance (swelling) and on drug dissolution using surface dissolution UV imaging. Acidic and basic pharmacopoeia (compendial) media were used to assess the role of varying pH on superdisintegrant performance and its effect on drug dissolution. A highly soluble (paracetamol) and a poorly soluble (carbamazepine) drug were used as model compounds and drug compacts and drug-excipient compacts were prepared for the dissolution experiments. The presence of a swelled SSG or CCS layer on the compact surface, due to the fast excipient hydration capacity, upon contact with dissolution medium was visualized. The swelling behaviour of superdisintegrants depended on excipient critical material attributes and the pH of the medium. Drug dissolution was faster in presence compared to superdisintegrant absence due to improved compact wetting or compact disintegration. The improvement in drug dissolution was less pronounced with increasing SSG viscosity or CCS particle size. Drug dissolution was slightly more complete in basic compared to acidic conditions in presence of the studied superdisintegrants for the highly soluble drug attributed to the increased excipient hydration capacity and the fast drug release through the swelled excipient structure. The opposite was observed for the poorly soluble drug as potentially the improvement in drug dissolution was compromised by drug release from the highly swelled structure. The use of multivariate data analysis revealed the influential role of excipient and drug properties on the impact of excipient variability on drug dissolution.

42 **Keywords:** excipient viscosity, excipient particle size, sodium starch glycolate, croscarmellose
43 sodium, excipient swelling, real – time surface dissolution UV imaging

44

1. Introduction

The identification and control of the critical material (i.e. excipient) properties are essential in the pharmaceutical Quality by Design (QbD) for the production of final products with the desirable critical quality attributes (Yu et al., 2014). Presence of superdisintegrants in oral solid dosage forms is essential for fast tablet disintegration and improved drug dissolution. Sodium starch glycolate (SSG) and croscarmellose sodium (CCS) (semisynthetic polymers of starch and cellulose, respectively) are commonly used as superdisintegrants in tablet manufacturing. The main mechanism by which superdisintegrants promote tablet disintegration is swelling (Quodbach and Kleinebudde, 2016). Swelling refers to the volume expansion of the superdisintegrant particles upon contact with water (Quodbach and Kleinebudde, 2016). The swelling mechanism of SSG and CCS has been confirmed with the use of real-time magnetic resonance imaging (Quodbach et al., 2014).

SSG and CCS are sodium salts and are present as a neutral form in acidic and ionized form in basic conditions. They derive from natural polymers after two main modification steps (carboxymethylation and crosslinking) of the natural polymer chains to improve excipient functionality (Quodbach and Kleinebudde, 2016). Firstly, carboxymethylation of the natural polymer backbone increases polymer hydrophilicity and allows water access into the excipient (Zhao and Augsburger, 2006). Secondly, as natural polymers are partially soluble, and their dissolution may increase the viscosity of the medium, crosslinking of the polymeric chains serves in decreasing the soluble content of the polymer. SSG is crosslinked through phosphate groups (Edge and Miller, 2005) while CCS through ester groups (Guest, 2005) (**Figure 1**). The superior performance of SSG and CCS as tablet disintegrants, compared to native polymers, is attributed to these two modification steps.

The extensive and fast swelling of SSG and CCS is demonstrated by the increase in their volume median diameter (average volumetric size) upon contact with water (123 μm upon

contact with water vs 35 μm of the dry excipient powder for SSG, 92 μm upon contact with water vs 45 μm of the dry excipient powder for CCS) and the amount of liquid water uptake (16 g/g and 10 g/g in 120 sec for SSG and CCS, respectively) (Zhao and Augsburger, 2005). The differences in the swelling capacity of SSG and CCS, despite their similar structure, have been attributed to the difference in their dimensional expansion (3-dimensional swelling for SSG, 2-dimensional swelling for CCS) (Rojas et al., 2012; Zhao and Augsburger, 2005) and their different crosslinking (the phosphate group of SSG, compared to the ester group of CCS, allows for more spacing between the polymeric chains) (Rojas et al., 2012). Molecular properties (degree of substitution, degree of crosslinking), particle properties (particle size distribution (PSD)) and level have been identified as potential critical material attributes for SSG and CCS affecting product performance (Zarmpi et al., 2017). Increasing the degree of substitution of SSG and CCS results in faster water uptake and excipient swelling, however optimum values need to be defined as high degrees of carboxymethylation may result in an increase in the viscosity of the medium (Zarmpi et al., 2017). Extensive swelling and faster disintegration have been reported when increasing the degree of crosslinking, particle size or level in formulations for SSG and CCS (Zarmpi et al., 2017).

The biopharmaceutical implications of superdisintegrant presence or variability on product performance are not well known. Gastrointestinal factors may impact the performance of superdisintegrants with pH being the most influential due to the ionization pattern of SSG and CCS. The hydration capacity of the acid excipient form in acidic media is lower compared to the ionized excipient form in basic media (acidic and basic media are defined based on the physiological pH range (Sjogren et al., 2014)) leading to reduced swelling in acidic conditions (Zhao and Augsburger, 2005). The % increase in the volume media diameter in water and 0.1 N HCl pH 1 was 251% and 43%, respectively for SSG and 104% and 51%, respectively for CCS (Zhao and Augsburger, 2005). The impact of superdisintegrants on product performance

relates also to drug properties. Interaction of cationic drugs with the carboxylic group of CCS can affect routine drug analysis. Loss of the active pharmaceutical ingredient (API) from a tablet formulation containing CCS during sample treatment can be expected, as low % recovery of drugs (metformin (Huang et al., 2006), escitalopram (Larsen and Melander, 2012)) from solutions in presence of CCS have been reported due to charge drug-excipient interactions. Delay in the dissolution of cationic drugs from immediate release tablets containing SSG and CCS has also been attributed to electrostatic drug-excipient interactions (Balasubramaniam et al., 2008).

Current approaches for assessing superdisintegrant performance and variability include the determination of: disintegration time of formulations, water uptake of powders/tablets, swelling volume of superdisintegrants, exerted force (force inside tablets that has to surpass the cohesive tablet forces) during tablet disintegration, dissolution rate of drugs, and size of generated particles after tablet disintegration (Quodbach and Kleinebudde, 2016). Real – time surface dissolution UV imaging is currently used in the pharmaceutical field providing additional information on disintegration/dissolution phenomena. UV dissolution imaging can be valuable in QbD approaches as it provides a mechanistic understanding into the surface events at the initial stages of drug dissolution and in early drug discovery to characterize new drug candidates (Kuentz, 2015; Niederquell and Kuentz, 2014). This technique utilizes a compact flow-cell integrated with a UV-vis camera and a pump for the infusion of the dissolution medium under laminar flow (Østergaard et al., 2014). The measured transmittance of light through the cell allows the characterization of the dissolving substance spatially and temporally and is useful for the identification of drug intrinsic dissolution rates, surface swelling/disintegration/dissolution phenomena, concentration gradients and microenvironmental pH changes (Gordon et al., 2013). Insights in the dissolution behaviour of APIs (Østergaard et al., 2014), excipients (Pajander et al., 2012) and their interplay (Colombo

et al., 2015; Hiew et al., 2018) have been provided with the use of real-time surface dissolution imaging.

The aims of this study were to assess the swelling performance of superdisintegrants with different potential critical material attributes and the impact and criticality of superdisintegrant variability on drug dissolution. Excipient characterization and drug dissolution studies in absence and presence of excipients were performed with the use of real-time surface dissolution UV imaging. The impact of excipient variability on excipient swelling and drug dissolution was studied by selecting three brands of SSG of different viscosity type and two brands of CCS of different PSD. A highly [paracetamol; Biopharmaceutical Classification System (BCS) class III (Kalantzi et al., 2006)] and a poorly soluble (carbamazepine; BCS class II (Kovacevic et al., 2009)) drug were used to assess the interplay of excipient variability and drug characteristics on drug dissolution. Studies were performed in acidic and basic compendial media to assess the role of pH on superdisintegrant swelling and drug dissolution.

2. Materials and Methods

2.1. Materials

APIs: Paracetamol (PRC, form I) was obtained from Fischer Scientific (UK). Carbamazepine (CBZ, form III) was purchased from Fagron (UK). Excipients: SSG brands: Glycolys LV [low viscosity (viscosity of aqueous solution at 60 min = 10.8 cP)] and Glycolys [high viscosity (viscosity of aqueous solution at 60 min = 20.9 cP)] (Roquette, France),. Explotab CLV [low viscosity (viscosity of aqueous solution at 60 min = 12.7 cP)] (JRS Pharma, USA) and CCS brands: AcDiSol [low particle size (d_{90} = 74.2 μ m)] (FMC, USA), Primellose [high particle size (d_{90} = 109.8 μ m)] (DFE Pharma, Germany) were obtained from the specified sources. Chemicals: Hydrochloric acid 36.5–38%, HPLC grade methanol were obtained from Sigma-Aldrich (UK). Sodium chloride, sodium hydroxide, potassium phosphate monobasic

were obtained from Fisher Scientific (UK). Water was ultra-pure (Milli-Q) laboratory grade. Filters: Polytetrafluoroethylene (PTFE) 13 mm filter 0.45 µm pore size were purchased from Fisher Scientific (UK).

2.2. Instrumentation

Sartorius BP 210 D balance (Sartorius UK Ltd, UK), Mettler Toledo SevenCompact S210 pH meter (Mettler Toledo, Switzerland), Vortex-Genie 2 vortex mixer (Scientific Industries Inc, USA), Agilent Technologies 1100 series HPLC system, (quaternary pump (G1311A), autosampler (G1313A), thermostatted column compartment (G1316A), diode array detector (G1329A) and a Chemstation software (Agilent Technologies, USA), Actipix SDI300 dissolution imaging system (Paraytec Ltd, UK) with an Actipix flow-through dissolution cartridge CADISS-2, Quickset Minor® torque screwdriver (Torqueleader, UK), Actipress 316 stainless steel press (Paraytec Ltd, UK).

2.3. Methods

2.3.1. Media used for *in vitro* dissolution studied

Compendial media (0.1 N HCl pH 1, phosphate buffer pH 6.8) were prepared according to the method described in the European Pharmacopeia (Ph.Eur., 2014).

2.3.2. Preparation of compacts

For the excipient characterization, 20 mg of each excipient were poured into the sample cup (stainless steel cylinder, inner diameter: 2 mm, height: 2.4 mm) and compacted using a manual press at a constant torque of 75 cNm for 5 min (Pajander et al., 2012). For the dissolution studies, compacts of pure APIs (paracetamol (PRC), carbamazepine (CBZ)) and compacts of superdisintegrants with the APIs were prepared. 10 mg of API (PRC, CBZ) were poured into the sample cup and compacts of pure API (drug compacts) were prepared using a manual press at a constant torque of 75 cNm for 5 min (Pajander et al., 2012). 10 mg of API

and 1 mg (2% w/w) of each excipient were prepared by vortexing (3 min) and poured into the sample cup. Compacts of superdisintegrants with APIs (drug-excipient compacts) were prepared using a manual press at a constant torque of 75 cNm for 5 min (Pajander et al., 2012).

2.3.3. *In vitro* real-time surface dissolution UV imaging

Real-time surface dissolution UV Imaging was performed using an Actipix SDI300 surface dissolution imaging system with an Actipix flow-through-type dissolution cartridge. The flow cell consisted of an Actipix cartridge fitted with a quartz cell (7 mm height, 4 mm width, 62 mm length) and a polyetheretherketone (PEEK) sample holder. The light source was a pulsed xenon lamp and a band-pass filter (detection wavelength \pm 10 nm) was used for the selection of the wavelength of interest. Dissolution medium was infused into the cell through a syringe pump. A temperature control unit was used to maintain constant temperature. The detection area of the UV imager was 9 mm \times 7 mm (1280 pixel \times 1024 pixel) with a pixel size of 7 μ m \times 7 μ m. Detailed representation of the instrument has been previously presented (Long et al., 2019; Østergaard et al., 2014).

For the excipient characterization, experiments were performed at 254 nm using stagnant conditions for 5 min at 37 °C in 0.1 N HCl pH 1 and phosphate buffer pH 6.8. *In vitro* drug dissolution experiments from drug compacts and drug-excipient compacts were performed at 280 nm using 1 mL/min flow rate for 20 min at 37 °C in 0.1 N HCl pH 1 and phosphate buffer pH 6.8. For both the excipient characterization experiments and *in vitro* drug dissolution studies, dark (10 s duration with the lamp turned off) and reference (10 s duration with the lamp turned on) images were recorded with the flow cell filled with dissolution medium in absence of compact. Data collection was initiated and after 60 s data recording was paused and the compacts were introduced into the cell. The system was flushed with dissolution media to avoid presence of air bubbles in the flow cell and data collection was resumed. Pixel intensities within

a designated quantification region were converted into absorbance values using the Actipix D100 software version 1.8.50805 (Paraytec Ltd, UK). In the *in vitro* drug dissolution experiments, the presence of the swelling excipients (SSG and CCS brands) in the quantification regions of the UV image resulted in increased scattering or physical blockage of light (Long et al., 2019). In these cases, the eluting sample was collected at 1 min intervals and the effluent samples were filtered through PTFE 0.45 µm pore size filters and analysed by HPLC. Filter adsorption studies were prior performed in triplicate for each drug and confirmed that there were no adsorption issues for the studied drugs on the filters used. All experiments were performed in triplicate.

2.3.4. Chromatographic conditions

Dissolution samples (effluent collection) were analysed by HPLC. Analytical HPLC procedures were modifications of already published methods for PRC (Gao et al., 2014) and CBZ (Vertzoni et al., 2006). A reversed-phase Spherisorb (Waters) C18 column (250 × 4.6 mm, 5 µm) was used for both drugs. For PRC, the mobile phase consisted of methanol and water 20:80 (v/v) and the temperature was kept constant at 20 °C. The injection volume was 20 µL and the detection wavelength was at 257 nm. For CBZ, the mobile phase was composed of methanol and water 60:40 (v/v) and the temperature was kept at 25 °C. The injection volume was 100 µL and the detection wavelength was at 285 nm. The flow rate was set at 1 mL/min for both drugs (isocratic flow). The elution times were 6 min and 4 min for PRC and CBZ, respectively. Drug quantification was made based on calibration curves. Standards were prepared from concentrated stock solution of drug dissolved in MeOH (PRC: 2 mg/mL, CBZ: 1 mg/mL). The range of the calibration curves were 10 – 300 µg/mL and 0.5 -50 µg/mL for PRC and CBZ, respectively.

2.3.5. Treatment of *in vitro* dissolution data

For the characterization of the swelling superdisintegrant behaviour, quantitative data of excipient concentration gradients cannot be obtained due to i. the insolubility of the studied polymers and ii. the fact that the high absorbance values recorded may be attributed to absorbance or scattering of light by the swelled polymer or physical blockage of light by undissolved polymer particles (Pajander et al., 2012). Only qualitative information of the rate and extent of swelling can be obtained by the absorbance gradients as a function of distance from the center of the sample cup. Absorbance values (Abs) were automatically calculated from pixel intensities using the Actipix D100 software version 1.8.50805 (Paraytec Ltd, UK) (zone dimensions of the images: 4.6 mm × 1.3 mm). The classification gradient maps (image gradients where changes of the z variable along the x and y directions are illustrated by changes in colour) depicting the swelling behaviour (absorbance values as a function of distance from the center of the sample cup) of the studied SSG and CCS brands in 0.1 N HCl pH 1 and phosphate buffer pH 6.8 were generated using SigmaPlot 13.0 (Systat Software Inc, USA). The cumulative % of drug dissolved was calculated based on the measured drug concentration in the samples (based on the HPLC analytical data) and the amount of drug in the compact. The dissolution profiles of the cumulative % of drug dissolved as a function time were constructed. Drug dissolution rates ($\mu\text{g}/\text{min}$) at each 1 min interval over the duration of the experiments were calculated based on the measured drug concentration in the samples (based on the HPLC analytical data) and the known flow rate of the dissolution experiments. Graphs depicting drug dissolution rates as a function of time (at 1 min intervals) were constructed and the standard deviation (SD) of the dissolution rates was presented in the midterm point of the sampling intervals.

The area under the curve (AUC) of the dissolution profiles up to last experimental time (20 min), calculated using the method of trapezoids, was used for the characterization of drug

dissolution. The Relative Effect (RE) of each superdisintegrant on drug dissolution was calculated based on equation 1:

$$RE = \frac{(AUC_T - AUC_C)}{AUC_C} \times 100 \quad \text{equation 1}$$

where AUC_C and AUC_T are the areas under the curve of the dissolution profiles of the control and test compact, respectively. Two sets of comparisons were performed. In the first set (set 1), the differences in drug dissolution between drug compacts and drug-excipient compacts in each medium were examined taking the AUCs of the dissolution profiles of the drug compact and the drug-excipient compact as control and test dissolution profiles, respectively. In the second set (set 2), differences in drug dissolution within acidic and basic conditions in each drug-excipient compact were investigated taking the AUCs of the dissolution profiles in acidic and basic conditions as the control and test dissolution profiles, respectively. The risk assessment of the impact of excipients on drug dissolution was evaluated by setting reference range criteria of -20% - 25% (FDA, 2002) on the REs of excipients on the AUCs of the dissolution profiles (this range was selected as a similar range is set in order to assess differences in drug exposure after oral administration; i.e. in bioequivalence studies). REs of excipients on the AUCs of the dissolution profiles outside these values (REs < -20% or REs > 25%) were considered potentially critical for oral drug performance.

2.3.6. Multivariate data analysis of *in vitro* dissolution data

Excipient REs on drug dissolution were correlated to excipient critical material attributes (viscosity for SSG, PSD for CCS), drug aqueous solubility ($\text{Drug}_{\text{aq.sol.}}$) and medium (acidic, basic) characteristics by multiple linear regression (MLR) using the XLSTAT software (Microsoft, USA). Two models for the REs of excipients on the AUCs of the dissolution profiles in presence of SSG (Model 1) and CCS (Model 2) were constructed. The evaluated variables for both models were all categorical and included: i. drug aqueous solubility

(Drug_{aq.sol.}) [0: poorly soluble, 1: highly soluble; based on the compound's BCS (Biopharmaceutical Classification System) classification (highly soluble: BCS Class I and III; poorly soluble: BCS Class II and IV) (FDA, 2017)], ii. medium (0: acidic, 1: basic), iii. excipient brand (0: low excipient property, 1: high excipient property; based on the measured viscosity values of SSG and the measured particle size (d_{90}) of the CCS brands). Excipient REs on the AUCs of the dissolution profiles (set 1, section 2.3.5) were used as the response. The selected interaction terms included each excipient brand combined with each drug aqueous solubility and medium characteristics (acidic, basic). The generated MLR models were assessed in terms of goodness of fit (R^2) and variance inflation factor (VIF). High R^2 values and VIF values < 5 were indications of successful models with absence of multicollinearity among the independent variables (Montgomery and Peck, 1992). Standardized coefficients were used to show the direction (positive or negative) and extent of each variable on the response. The significance of the variables was assessed by the p values ($p < 0.05$ were considered the most significant in the model (Montgomery and Peck, 1992)). A 95% confidence interval was used.

3. Results and Discussion

3.1. Characterization of the swelling behaviour of superdisintegrants using real-time surface dissolution UV Imaging

The studied excipient types and brands have been previously characterized in terms of viscosity for SSG and PSD for CCS (Zarmpi et al., 2019). The viscosity after 60 min of the aqueous dispersions of Glycolys LV (10.8 cP) and Explotab CLV (12.7 cP) was lower compared to Glycolys (20.9 cP), due to their higher degree of crosslinking and lower soluble material content (Shah and Augsburger, 2001). Differences in the PSD of the CCS brands were

identified, as AcDiSol comprised of smaller particles (d10: 12.8 μm , d50: 31.9 μm , d90: 74.2 μm) compared to Primellose (d10: 21.8 μm , d50: 52.2 μm d90: 109.8 μm).

Surface dissolution UV imaging was used to study the swelling performance of SSG and CCS in simple buffers and UV images of the excipient swelling upon contact with the dissolution media are presented in **Supplementary Figure 1**. The swelling behaviour of the studied superdisintegrants as a function of time and distance from the centre of the sample cup in 0.1 N HCl pH 1 is presented in **Figure 2**. Intense signals at the compact location are indications of dense swollen polymeric structures (Colombo et al., 2015), as the high absorbance recorded are attributed to light scattering by the swelled superdisintegrants or physical blockage of light by undissolved excipient particles (as explained in section 2.3.5.). The fast excipient swelling was demonstrated as all the studied superdisintegrants swelled at a distance of 1.2 mm from the centre of the sample cup at approximately 20 – 40 s irrespective of excipient type or brand. For SSG, Glycolys exhibited lower absorbance values ($\text{Abs} \approx 1.0 - 1.2 \text{ AU}$) compared to Glycolys LV and Explotab CLV ($\text{Abs} \approx 1.2 - 1.6 \text{ AU}$) probably due to the higher soluble content of high viscosity brands (Shah and Augsburger, 2001). For CCS, the higher absorbance values of Primellose ($\text{Abs} \approx 1.4 - 1.6 \text{ AU}$) compared to AcDiSol ($\text{Abs} \approx 1.0 - 1.2 \text{ AU}$) can be attributed to the pronounced physical blockage of light by larger particles (Van Eerdenbrugh et al., 2011).

The swelling behaviour of the studied superdisintegrants as a function of time and distance from the centre of the sample cup in phosphate buffer pH 6.8 is presented in **Figure 3**. Slightly faster excipient swelling in phosphate buffer pH 6.8 ($< 20 \text{ s}$) was observed compared to 0.1 N HCl pH 1 (20 – 40 s) explained by the higher liquid uptake (0.1 N HCl pH 1: approximately 5 g/g liquid uptake by SSG and CCS after 2 min, water: 18 g/g and 10 g/g liquid uptake by SSG and CCS, respectively after 2 min (Zhao and Augsburger, 2005)) and excipient swelling of the ionized excipient form in basic media (Zhao and Augsburger, 2005). The

absorbance values of the studied brands were lower in phosphate buffer pH 6.8 (SSG brands: 0.6 – 1.2 AU, CCS brands: 1.0 – 1.4 AU) compared to 0.1 N HCl pH 1 (SSG brands: 1.0 – 1.6 AU, CCS brands: 1.0 – 1.6 AU). We hypothesize that the lower absorbance values in the basic compared to the acidic medium relate to the higher excipient swelling of the ionized excipient forms in phosphate buffer pH 6.8 (as compared to the unionized excipient forms in 0.1 N HCl pH 1), as the higher spacing of the swelled polymeric chains (Rojas et al., 2012) could decrease the scattering or physical blockage of light. Differences in the absorbance values are not observed within the studied SSG brands (Abs \approx 0.6 – 1.0 AU). For CCS, lower absorbance values were observed for AcDiSol (Abs \approx 1.0 – 1.2 AU) attributed to its lower particle size compared to Primellose (Abs \approx 1.2 – 1.4 AU) [24]. The lower absorbance values of the SSG compared to the CCS brands in phosphate buffer pH 6.8 can indicate a more extensive swelling by SSG, due to the differences in the dimensional expansion (3 dimensional swelling (semispherical particles) for SSG and 2 dimensional swelling (fibrous particles) for CCS upon contact with simulated intestinal fluid have been reported (Rojas et al., 2012)) and type of crosslinking (phosphate groups for SSG, ester group for CCS) between the two excipient types (Rojas et al., 2012). The observed differences in excipient performance in the studied media indicate that differences in tablet disintegration between the stomach and the small intestine are anticipated (due to the differences in the pH of these two compartments) and could potentially implicate product performance and drug bioavailability.

3.2. Impact of SSG variability on drug dissolution using surface dissolution UV Imaging

3.2.1. Highly soluble drug (PRC)

The dissolution profiles and dissolution rates of PRC from drug compacts (control) and drug-SSG compacts in 0.1 N HCl pH 1 and phosphate buffer pH 6.8 are presented in **Figure**

4. Approximately 5% of PRC dissolved from the drug compact in 20 min in both media. The % of drug dissolved in 20 min from the drug-SSG compacts was increased in 0.1 N HCl pH 1 (21%, 23% and 25% of drug dissolved in the presence of Glycolys LV, Explotab CLV and Glycolys, respectively) and in phosphate buffer pH 6.8 (22%, 27% and 21% of drug dissolved in the presence of Glycolys LV, Explotab CLV and Glycolys, respectively). The dissolution rate of PRC from drug compacts was slow during the experiments in both media studied (dissolution rates of approximately 20 µg/min and 17 µg/min in 0.1 N HCl pH 1 and phosphate buffer pH 6.8 at 20 min, respectively). Drug dissolution from drug-SSG compacts was faster compared to drug dissolution from drug compacts in the studied media, especially at early time points (1 – 5 min), as indicated by the increased dissolution rates of PRC in excipient presence (dissolution rates of approximately 200 µg/min from compacts containing Glycolys LV, Explotab CLV and Glycolys at 5 min in both media). This could be explained by the fast excipient hydration and swelling (excipient swelling at a distance of 1.2 mm from the centre of the sample cup within the first 40s, section 3.1) improving compact wetting (Onuki et al., 2018). Compact disintegration may also have contributed to the faster drug dissolution from drug-excipient compacts compared to drug compacts, as spread particles around the compact surface were observed after the end of each experiment only for the drug-excipient compacts. Comparison of the AUCs of the dissolution profiles revealed that drug dissolution was more complete from the drug-excipient compacts compared to drug dissolution from the drug compacts (REs > 25%) (**Figure 5a**). Differences in PRC dissolution from drug-SSG compacts in acidic and basic conditions for the studied SSG brands were not observed (REs of approximately 5%, 20% and -20% for Glycolys LV, Explotab CLV and Glycolys, respectively). The observed minor REs indicate that the pH-dependent swelling performance of SSG (section 3.1) may not significantly affect the dissolution of a highly soluble drug between acidic and basic conditions.

3.2.2. Poorly soluble drug (CBZ)

The dissolution profiles and dissolution rates of CBZ from drug compacts (control) and drug-SSG compacts in 0.1 N HCl pH 1 and phosphate buffer pH 6.8 are presented in **Figure 6**. Approximately 0.1% of CBZ dissolved from the drug compact in 20 min in both 0.1 N HCl pH and phosphate buffer pH 6.8. In 0.1 N HCl pH 1, 2.3%, 1.6% and 1.3% of drug dissolved in 20 min in presence of Glycolys LV, Explotab CLV and Glycolys, respectively. The % of CBZ dissolved in excipient presence in phosphate buffer pH 6.8 in 20 min was similar between the different drug-excipient compacts (approximately 1.5% of CBZ dissolved from drug-excipient compact containing Glycolys LV, Explotab CLV, Glycolys). The rate of drug dissolution from the drug compact was slow in both sets of media (dissolution rates of approximately 0.5 µg/min at 20 min in 0.1 N HCl pH 1 and phosphate buffer pH 6.8). CBZ dissolution was faster in SSG presence, especially at early time points (1 - 5 min), potentially due to the fast excipient swelling or compact disintegration (as explained in the case of PRC). In 0.1 N HCl pH 1, the dissolution rates of CBZ from drug-excipient compacts were 13 µg/min, 8.6 µg/min and 6.2 µg/min at 5 min in presence of Glycolys LV, Explotab CLV and Glycolys, respectively. The lower amount of drug dissolved in presence of Glycolys compared to the low viscosity brands (Glycolys LV, Explotab CLV) may be explained by the increase in the viscosity of the gel around the compact by high viscosity Glycolys (Quodbach and Kleinebudde, 2016). The pronounced differences in the CBZ dissolution rates from compacts containing the low and high viscosity SSG brands are diminished at late points. Faster CBZ dissolution in presence compared to absence of excipient was also observed in phosphate buffer pH 6.8, with the dissolution rates from the three drug-excipient compacts being similar (CBZ dissolution rates of approximately 7 µg/min at 5 min in presence of the three studied SSG brands). CBZ dissolution in presence of excipient was more complete compared to the excipient absence (REs > 25%) (**Figure 5a**). Differences in drug dissolution from drug-

excipient compacts between acidic and basic conditions were observed. For the low viscosity brands (Glycolys LV, Explotab CLV), the REs on the AUCs of the dissolution profiles between acidic and basic conditions were negative (REs of -45% and -20% for Glycolys LV and Explotab CLV, respectively), indicating that the improvement in CBZ dissolution is less pronounced in phosphate buffer pH 6.8 compared to 0.1 N HCl pH 1. As superdisintegrants swell more extensively in basic compared to acidic conditions due to their ionization (Rojas et al., 2012), the presence of a highly swelled layer on top of the sample cup may add a physical or diffusive barrier for the release of poorly soluble drugs (Long et al., 2019), despite the faster polymer water uptake in basic conditions (as explained previously in section 3.1). The swelling of the high viscosity Glycolys is as well more extensive in basic compared to acidic conditions, however comparison of CBZ dissolution profiles from compacts containing Glycolys between basic and acidic media reveal slightly more complete dissolution in phosphate buffer pH 6.8 (REs of 30%). This positive RE on the AUCs of the dissolution profiles may relate to the gelling effects of Glycolys (Quodbach and Kleinebudde, 2016) and the slower CBZ dissolution observed in 0.1 N HCl pH 1 (compared to the other two excipient brands).

3.3. Impact of CCS variability on drug dissolution using surface dissolution UV Imaging

3.3.1. Highly soluble drug (PRC)

The dissolution profiles and dissolution rates of PRC from drug compacts (control) and drug-CCS compacts in 0.1 N HCl pH 1 and phosphate buffer pH 6.8 are presented in **Figure 7**. A higher % of drug dissolved in 20 min was observed in excipient presence in 0.1 N HCl pH 1 (AcDiSol: 23%, Primellose: 14%) and phosphate buffer pH 6.8 (AcDiSol: 25%, Primellose: 26%) compared to the % of PRC dissolved from the drug compact (5% of drug dissolved in 20 min). Faster drug dissolution was revealed in excipient presence compared to

excipient absence in both media which may be explained by the enhancement in compact wetting or compact disintegration due to the hydrophilicity and swelling of CCS (Quodbach and Kleinebudde, 2016). Differences in drug dissolution rates from the studied drug-CCS compacts were observed at early time points in 0.1 N HCl pH 1 as the dissolution rate of PRC was lower in presence of Primellose (98 µg/min of drug dissolved at 5 min) compared to AcDiSol (182 µg/min of drug dissolved at 5 min), probably due to the presence of larger excipient particles (Primellose) on top of the compact surface (section 3.1). In phosphate buffer pH 6.8 similar drug dissolution was observed between the drug-CCS compacts containing AcDiSol and Primellose (dissolution rates of approximately 200 µg/min in presence of both CCS brands at 5 min). At late time points, the dissolution rate of PRC gradually decreased in presence of the CCS brands in both media and any differences in drug dissolution between the studied CCS brands were diminished. Comparison of the AUCs of the dissolution profiles of the drug and drug-CCS compacts revealed significantly more complete dissolution from compacts containing excipient (REs > 25%) (**Figure 5b**). Differences in drug dissolution from drug-AcDiSol compacts between acidic and basic conditions were not observed, as revealed by the REs of AcDiSol on the AUCs of the dissolution profiles between acidic and basic conditions (RE = 10%). Drug dissolution from the drug-Primellose compacts was significantly more complete in phosphate buffer pH 6.8 compared to 0.1 N HCl pH (RE = 97%), potentially due to the presence of larger excipient particles in 0.1 N HCl pH 1.

3.3.2. Poorly soluble drug (CBZ)

The dissolution profiles and dissolution rates of CBZ from drug compacts and drug-CCS compacts in 0.1 N HCl pH 1 and phosphate buffer pH 6.8 are presented in **Figure 8**. CBZ dissolution reached approximately 1.8% and 1.5% from compacts containing AcDiSol and Primellose, respectively in 0.1 N HCl pH 1 and 1.3% and 1.0% in phosphate buffer pH 6.8. The fast excipient swelling at early time points (section 3.1) resulted in faster drug dissolution

from drug-CCS compacts compared to the drug compacts in both sets of media, especially at early time points. Drug dissolution was slower in presence of Primellose (7 µg/min and 5 µg/min in acidic and basic conditions, respectively) compared to AcDiSol (9 µg/min and 7 µg/min in the acidic and basic medium, respectively), probably due to the presence of larger excipient particles (Primellose) on top of the compact surface (section 3.1). Differences in drug dissolution between the studied brands were smaller at late time points. In presence of excipient, drug dissolution was significantly more complete compared to the control sample in both experimental conditions (REs > 25%) (**Figure 5b**). The enhancement in CBZ dissolution by CCS presence was more pronounced in acidic compared to basic conditions (REs on the AUCs of the dissolution profiles between acidic and basic conditions of -30% and -20% for AcDiSol and Primellose, respectively). The faster water uptake of the excipients in basic media (Rojas et al., 2012) would be expected to result in faster drug dissolution due to the improved compact wetting, however this is not observed as potentially the presence of a swelled layer on top of the compact surface created a physical or diffusive barrier delaying drug release (Long et al., 2019).

For the dissolution experiments in the absence of excipients, high variability (coefficient of variation (CV%) > 20%) was observed in some cases only at the first 3 min, and a lower variability was observed in later time points (CV% < 20%). For the dissolution experiments in excipient presence, cases of increased variability were identified (15% < CV% < 70% and 15% < CV% < 50% at early and late time points, respectively) that may relate to the heterogeneous nature of the physical mixtures (Koester et al., 2003a; Koester et al., 2003b; Zarmpi et al., 2019). The preparation process of the physical mixtures could be further optimized in future studies along with the use of more replicates.

3.4. Multivariate data analysis of *in vitro* dissolution data

The standardized coefficients of the variables for the SSG and CCS model are presented in **Figure 9**. The two models showed a good fit (SSG: $R^2 = 0.5$, CCS: $R^2 = 0.5$). For SSG, excipient brand (negative effect, $p < 0.05$), $\text{Drug}_{\text{aq.sol.}}$ (negative effect, $p < 0.05$) and medium (negative effect, $p < 0.05$) were the critical variables in the model. The negative effect of the excipient brand indicates that increasing the viscosity type of SSG resulted in less pronounced dissolution enhancement compared to the low viscosity SSG brands. Enhanced compact wetting by low viscosity SSG brands is expected due to their faster water uptake and higher swelling (Abraham et al., 2016). Formation of gelling layer by high viscosity SSG brands which delays drug dissolution (Quodbach and Kleinebudde, 2016) could also explain this finding. The impact of varying SSG viscosity was more pronounced for the poorly soluble drug, indicated by the significance of the variable $\text{Drug}_{\text{aq.sol.}}$ in the model, as poorly soluble drugs will benefit more by an improvement in compact wetting. The negative effect of the variable medium reveals the pronounced enhancement in drug dissolution by SSG presence in acidic compared to basic conditions (especially, for the poorly soluble drug).

For CCS, excipient brand (negative effect, $p < 0.05$) and $\text{Drug}_{\text{aq.sol.}}$ (negative effect, $p < 0.05$) were critical variables in the model. Increasing the particle size of CCS will result in less pronounced improvement in drug dissolution probably due to the formation of physical or diffusive barrier for drug dissolution by larger excipient particles. The negative effect of the variable $\text{Drug}_{\text{aq.sol.}}$ indicates that the improved wetting or compact disintegration by CCS presence will contribute more to the dissolution of poorly soluble drugs. The multivariate data analysis revealed that CCS variability may be critical for the initial stages of drug dissolution.

4. Conclusions

Superdisintegrant variability and interchangeability may be challenging for oral product performance, as the presence of superdisintegrants in pharmaceutical formulations directly

affects drug dissolution. In this study, the use of surface dissolution UV imaging allowed the semi-qualitative analysis of SSG and CCS swelling and their impact on drug dissolution. The fast swelling ability of SSG and CCS was confirmed, which depended on the critical excipient material attributes and the pH of the dissolution medium. These results reveal that SSG and CCS should not be considered interchangeable with each other in oral solid dosage forms. Presence of superdisintegrants in compacts containing highly and poorly soluble compounds resulted in significantly faster drug dissolution for both drugs probably due to the enhanced compact wetting or compact disintegration by the hydrophilic excipients. Changing excipients with varying material properties needs to be carefully consider in oral drug development as the different excipient critical material attributes affected the extent of drug dissolution (pronounced dissolution enhancement was observed by low viscosity SSG or low particle size CCS brands, especially for the poorly soluble drug). The potential biopharmaceutical implications of superdisintegrants were revealed, as in superdisintegrant presence, an interplay between drug aqueous solubility and medium characteristics was found that could affect product performance (highly soluble drug: faster drug dissolution in basic compared to acidic media due to the increased excipient hydration capacity; poorly soluble drug: slower drug dissolution in basic compared to acidic media potentially due to the presence of a swollen excipient structure on top of the compact). SSG viscosity type, CCS particle size and drug aqueous solubility were considered critical biopharmaceutical factors affecting the performance and the impact of superdisintegrant variability on drug dissolution. It is concluded that excipient variability can be challenging for oral drug performance and that biopharmaceutical considerations need to be taken into account when changes in excipient brands/grades are necessary in oral product development. Further studies to assess the impact and interplay of other superdisintegrant properties using a wide range of compounds would be beneficial in delineating the impact of excipient variability on drug dissolution.

508 **Acknowledgements**

509 The authors would like to acknowledge AstraZeneca and the University of Bath for funding
510 the current project.

References

- Abraham, A., Olusanmi, D., Ilott, A.J., Good, D., Murphy, D., McNamara, D., Jerschow, A., Mantri, R.V., 2016. Correlation of Phosphorus Cross-Linking to Hydration Rates in Sodium Starch Glycolate Tablet Disintegrants Using MRI. *J. Pharm. Sci.* 105, 1907-1913, <https://doi.org/10.1016/j.xphs.2016.03.025>.
- Balasubramaniam, J., Bindu, K., Rao, V.U., Ray, D., Halder, R., Brzezczko, A.W., 2008. Effect of Superdisintegrants on Dissolution of Cationic Drugs. *Dissolut. Technol.* 15, 18-25, <https://doi.org/10.14227/DT150208P18>.
- Colombo, S., Brisander, M., Haglöf, J., Sjövall, P., Andersson, P., Østergaard, J., Malmsten, M., 2015. Matrix effects in nilotinib formulations with pH-responsive polymer produced by carbon dioxide-mediated precipitation. *Int. J. Pharm.* 494, 205-217, <https://doi.org/10.1016/j.ijpharm.2015.08.031>.
- Edge, S., Miller, R.W., 2005. Sodium Starch Glycolate, in: Rowe, R.C., Sheskey, P.J., Owen, S.C. (Eds.), *Handbook of Pharmaceutical Excipients*, 5th ed. Pharmaceutical Press and American Pharmacists Association, 1 Lambeth High Street, London SE1 7JN, UK 100 South Atkinson Road, Suite 206, Grayslake, IL 60030-7820, USA 1 2215 Constitution Avenue, NW Washington, DC 20037-2985, USA, pp. 701-704.
- FDA, 2002. Guidance For Industry: Bioavailability And Bioequivalence Studies For Orally Administered Drug Products - General Considerations.
- FDA, 2017. Waiver of In Vivo Bioavailability and Bioequivalence Studies for Immediate-Release Solid Oral Dosage Forms Based on a Biopharmaceutics Classification System Guidance for Industry.
- Gao, N., Qi, B., Liu, F.J., Fang, Y., Zhou, J., Jia, L.J., Qiao, H.L., 2014. Inhibition of baicalin on metabolism of phenacetin, a probe of CYP1A2, in human liver microsomes and in rats. *PLoS One* 9, e89752, <https://doi.org/10.1371/journal.pone.0089752>.

536 Gordon, S., Naelapää, K., Rantanen, J., Selen, A., Müllertz, A., Østergaard, J., 2013. Real-time
 537 dissolution behavior of furosemide in biorelevant media as determined by UV imaging. *Pharm.*
 538 *Dev. Technol.* 18, 1407-1416, <https://doi.org/10.3109/10837450.2012.737808>.
 539 Guest, R.T., 2005. Croscarmellose Sodium, in: Rowe, R.C., Sheskey, P.J., Owen, S.C. (Eds.),
 540 Handbook of Pharmaceutical Excipients, 5th ed. Pharmaceutical Press and American
 541 Pharmacists Association, 1 Lambeth High Street, London SE1 7JN, UK 100 South Atkinson
 542 Road, Suite 206, Grayslake, IL 60030-7820, USA 1 2215 Constitution Avenue, NW
 543 Washington, DC 20037-2985, USA, pp. 211-213.
 544 Hiew, T.N., Alaudin, M.I.B., Chua, S.M., Heng, P.W.S., 2018. A study of the impact of
 545 excipient shielding on initial drug release using UV imaging. *Int. J. Pharm.* 553, 229-237,
 546 <https://doi.org/10.1016/j.ijpharm.2018.10.040>.
 547 Huang, W.X., Desai, M., Tang, Q., Yang, R., Vivilecchia, R.V., Joshi, Y., 2006. Elimination
 548 of metformin–croscarmellose sodium interaction by competition. *Int. J. Pharm.* 311, 33-39,
 549 <http://dx.doi.org/10.1016/j.ijpharm.2005.12.017>.
 550 Kalantzi, L., Reppas, C., Dressman, J.B., Amidon, G.L., Junginger, H.E., Midha, K.K., Shah,
 551 V.P., Stavchansky, S.A., Barends, D.M., 2006. Biowaiver monographs for immediate release
 552 solid oral dosage forms: acetaminophen (paracetamol). *J. Pharm. Sci.* 95, 4-14,
 553 <https://doi.org/10.1002/jps.20477>.
 554 Koester, L.S., Mayorga, P., Bassani, V.L., 2003a. Carbamazepine/betaCD/HPMC solid
 555 dispersions. I. Influence of the spray-drying process and betaCD/HPMC on the drug dissolution
 556 profile. *Drug Dev Ind Pharm* 29, 139-144, 10.1081/ddc-120016721.
 557 Koester, L.S., Mayorga, P., Pereira, V.P., Petzhold, C.L., Bassani, V.L., 2003b.
 558 Carbamazepine/betaCD/HPMC solid dispersions. II. Physical characterization. *Drug Dev Ind*
 559 *Pharm* 29, 145-154, 10.1081/ddc-120016722.

560 Kovacevic, I., Parojcic, J., Homsek, I., Tubic-Grozdanis, M., Langguth, P., 2009. Justification
 561 of biowaiver for carbamazepine, a low soluble high permeable compound, in solid dosage
 562 forms based on IVIVC and gastrointestinal simulation. *Mol. Pharm.* 6, 40-47,
 563 <https://doi.org/10.1021/mp800128y>.
 564 Kuentz, M., 2015. Analytical technologies for real-time drug dissolution and precipitation
 565 testing on a small scale. *J. Pharm. Pharmacol.* 67, 143-159, <https://doi.org/10.1111/jphp.12271>.
 566 Larsen, J., Melander, C., 2012. Study of interaction between croscarmellose and escitalopram
 567 during sample preparation. *Drug Dev. Ind. Pharm.* 38, 1195-1199,
 568 <https://doi.org/10.3109/03639045.2011.643896>.
 569 Long, C.M., Tang, K., Chokshi, H., Fotaki, N., 2019. Surface Dissolution UV Imaging for
 570 Investigation of Dissolution of Poorly Soluble Drugs and Their Amorphous Formulation.
 571 *AAPS Pharm. Sci. Tech.* 20, 113, <https://doi.org/10.1208/s12249-019-1317-z>.
 572 Montgomery, D.C., Peck, E.A., 1992. Introduction to Linear Regression Analysis. John Wiley
 573 and Sons, Inc.
 574 Niederquell, A., Kuentz, M., 2014. Biorelevant dissolution of poorly soluble weak acids
 575 studied by UV imaging reveals ranges of fractal-like kinetics. *Int. J. Pharm.* 463, 38-49,
 576 <https://doi.org/10.1016/j.ijpharm.2013.12.049>.
 577 Onuki, Y., Kosugi, A., Hamaguchi, M., Marumo, Y., Kumada, S., Hirai, D., Ikeda, J., Hayashi,
 578 Y., 2018. A comparative study of disintegration actions of various disintegrants using
 579 Kohonen's self-organizing maps. *Drug Deliv. Sci. Technol.* 43, 141-148,
 580 <https://doi.org/10.1016/j.jddst.2017.10.002>.
 581 Østergaard, J., Lenke, J., Jensen, S.S., Sun, Y., Ye, F., 2014. UV Imaging for *In Vitro*
 582 Dissolution and Release Studies: Initial experiences. *Dissolut. Technol.* 21, 27-38,
 583 <https://doi.org/10.14227/DT210414P27>.

584 Pajander, J., Baldursdottir, S., Rantanen, J., Østergaard, J., 2012. Behaviour of HPMC
 585 compacts investigated using UV-imaging. *Int. J. Pharm.* 427, 345-353,
 586 <http://dx.doi.org/10.1016/j.ijpharm.2012.02.034>.
 587 Ph.Eur., 2014. European Pharmacopeia 8.0: 5.17 Recommendations on Methods for Dosage
 588 Form Testing. Strasbourg: Council of Europe, pp. 727-729.
 589 Quodbach, J., Kleinebudde, P., 2016. A critical review on tablet disintegration. *Pharm. Dev.*
 590 *Technol.* 21, 763-774, <https://doi.org/10.3109/10837450.2015.1045618>.
 591 Quodbach, J., Moussavi, A., Tammer, R., Frahm, J., Kleinebudde, P., 2014. Tablet
 592 Disintegration Studied by High-Resolution Real-Time Magnetic Resonance Imaging. *J. Pharm.*
 593 *Sci.* 103, 249-255, <https://doi.org/10.1002/jps.23789>.
 594 Rojas, J., Guisao, S., Ruge, V., 2012. Functional Assessment of Four Types of Disintegrants
 595 and their Effect on the Spironolactone Release Properties. *AAPS Pharm. Sci. Tech.* 13, 1054-
 596 1062, <https://doi.org/10.1208/s12249-012-9835-y>.
 597 Shah, U., Augsburger, L., 2001. Evaluation of the functional equivalence of crospovidone NF
 598 from different sources. I. Physical characterization. *Pharm. Dev. Technol.* 6, 39-51,
 599 <https://doi.org/10.1081/pdt-100000012>.
 600 Sjogren, E., Abrahamsson, B., Augustijns, P., Becker, D., Bolger, M.B., Brewster, M.,
 601 Brouwers, J., Flanagan, T., Harwood, M., Heinen, C., Holm, R., Juretschke, H.P., Kubbinga,
 602 M., Lindahl, A., Lukacova, V., Munster, U., Neuhoff, S., Nguyen, M.A., Peer, A., Reppas, C.,
 603 Hodjegan, A.R., Tannergren, C., Weitschies, W., Wilson, C., Zane, P., Lennernas, H.,
 604 Langguth, P., 2014. In vivo methods for drug absorption - comparative physiologies, model
 605 selection, correlations with in vitro methods (IVIVC), and applications for
 606 formulation/API/excipient characterization including food effects. *Eur. J. Pharm. Sci.* 57, 99-
 607 151, <https://doi.org/10.1016/j.ejps.2014.02.010>.

608 Van Eerdenbrugh, B., Alonzo, D.E., Taylor, L.S., 2011. Influence of Particle Size on the
 609 Ultraviolet Spectrum of Particulate-Containing Solutions: Implications for In-Situ
 610 Concentration Monitoring Using UV/Vis Fiber-Optic Probes. *Pharm. Res.* 28, 1643-1652,
 611 <https://doi.org/10.1007/s11095-011-0399-4>.
 612 Vertzoni, M.V., Reppas, C., Archontaki, H.A., 2006. Sensitive and simple liquid
 613 chromatographic method with ultraviolet detection for the determination of nifedipine in canine
 614 plasma. *Analytica Chimica Acta* 573-574, 298-304, <https://doi.org/10.1016/j.aca.2006.03.037>.
 615 Yu, L.X., Amidon, G., Khan, M.A., Hoag, S.W., Polli, J., Raju, G.K., Woodcock, J., 2014.
 616 Understanding pharmaceutical quality by design. *AAPS J.* 16, 771-783,
 617 <https://doi.org/10.1208/s12248-014-9598-3>.
 618 Zarmpi, P., Flanagan, T., Meehan, E., Mann, J., Fotaki, N., 2017. Biopharmaceutical aspects
 619 and implications of excipient variability in drug product performance. *Eur. J. Pharm.*
 620 *Biopharm.* 111, 1-15, <http://dx.doi.org/10.1016/j.ejpb.2016.11.004>.
 621 Zarmpi, P., Flanagan, T., Meehan, E., Mann, J., Fotaki, N., 2019. Biopharmaceutical
 622 understanding of excipient variability on drug apparent solubility based on drug
 623 physicochemical properties. Case study: Superdisintegrants. *AAPS J.*
 624 <http://dx.doi.org/10.1208/s12248-019-0406-y>.
 625 Zhao, N., Augsburger, L., 2006. The Influence of Product Brand-to-Brand Variability on
 626 Superdisintegrant Performance A Case Study with Croscarmellose Sodium. *Pharm. Dev. Tech.*
 627 11, 179-185, <https://doi.org/10.1080/10837450600561281>.
 628 Zhao, N., Augsburger, L.L., 2005. The influence of swelling capacity of superdisintegrants in
 629 different pH media on the dissolution of hydrochlorothiazide from directly compressed tablets.
 630 *AAPS Pharm.Sci.Tech.* 6, 120-126, <https://doi.org/10.1208/pt060119>.

Figure captions

Figure 1: Chemical structure of a. Sodium Starch Glycolate and b. Croscarmellose Sodium (ChemDraw Professional 15)

Figure 2: Absorbance values (Abs) of the studied superdisintegrant types and brands as a function of distance from the center of the sample cup (mm) in 0.1 N HCl pH 1 (SDi1, 0 mL/min, 37 °C, 254 nm) presented up to 2.5 min.

Figure 3: Absorbance values (Abs) of the studied superdisintegrant types and brands as a function of distance from the center of the sample cup (mm) in phosphate buffer pH 6.8 (SDi1, 0 mL/min, 37 °C, 254 nm) up to 2.5 min.

Figure 4: Cumulative % dissolved (top) and dissolution rates (bottom) of PRC from compacts in a. 0.1 N HCl pH 1 and b. phosphate buffer pH 6.8 using real-time surface dissolution UV imaging (SDi1, 1 mL/min, 37°C) in absence (control: black circles/colour) and presence of the studied SSG brands (Glycolys LV: green squares/colour, Explotab CLV: blue diamonds/colour, Glycolys: red triangles/colour). (Mean \pm SD, n =3)

Figure 5: a. Relative effects of excipients on the AUCs of the dissolution profiles for a. PRC and b. CBZ in presence of the studied SSG brands (Glycolys LV: green colour, Explotab CLV: blue colour, Glycolys: red colour) in 0.1 N HCl pH 1 and phosphate buffer pH 6.8. b. Relative effects of excipients on the AUCs of the dissolution profiles for a. PRC and b. CBZ in presence of the studied CCS brands (AcDiSol: blue colour, Primellose: red colour) in 0.1 N HCl pH 1 and phosphate buffer pH 6.8.

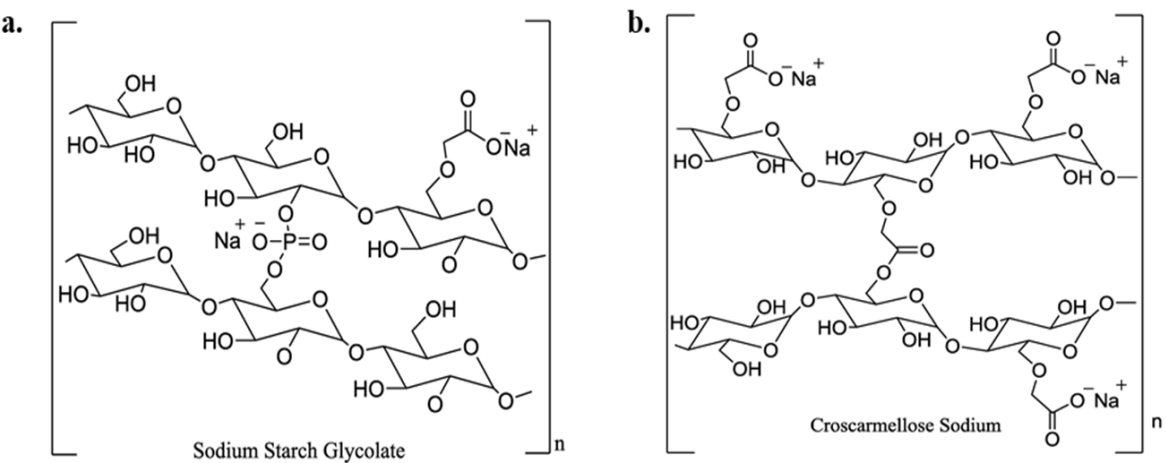
Figure 6: Cumulative % dissolved (top) and dissolution rates (bottom) of CBZ from compacts in a. 0.1 N HCl pH 1 and b. phosphate buffer pH 6.8 using real-time surface dissolution UV imaging (SDi1, 1 mL/min, 37°C) in absence (control: black circles/colour) and presence of the

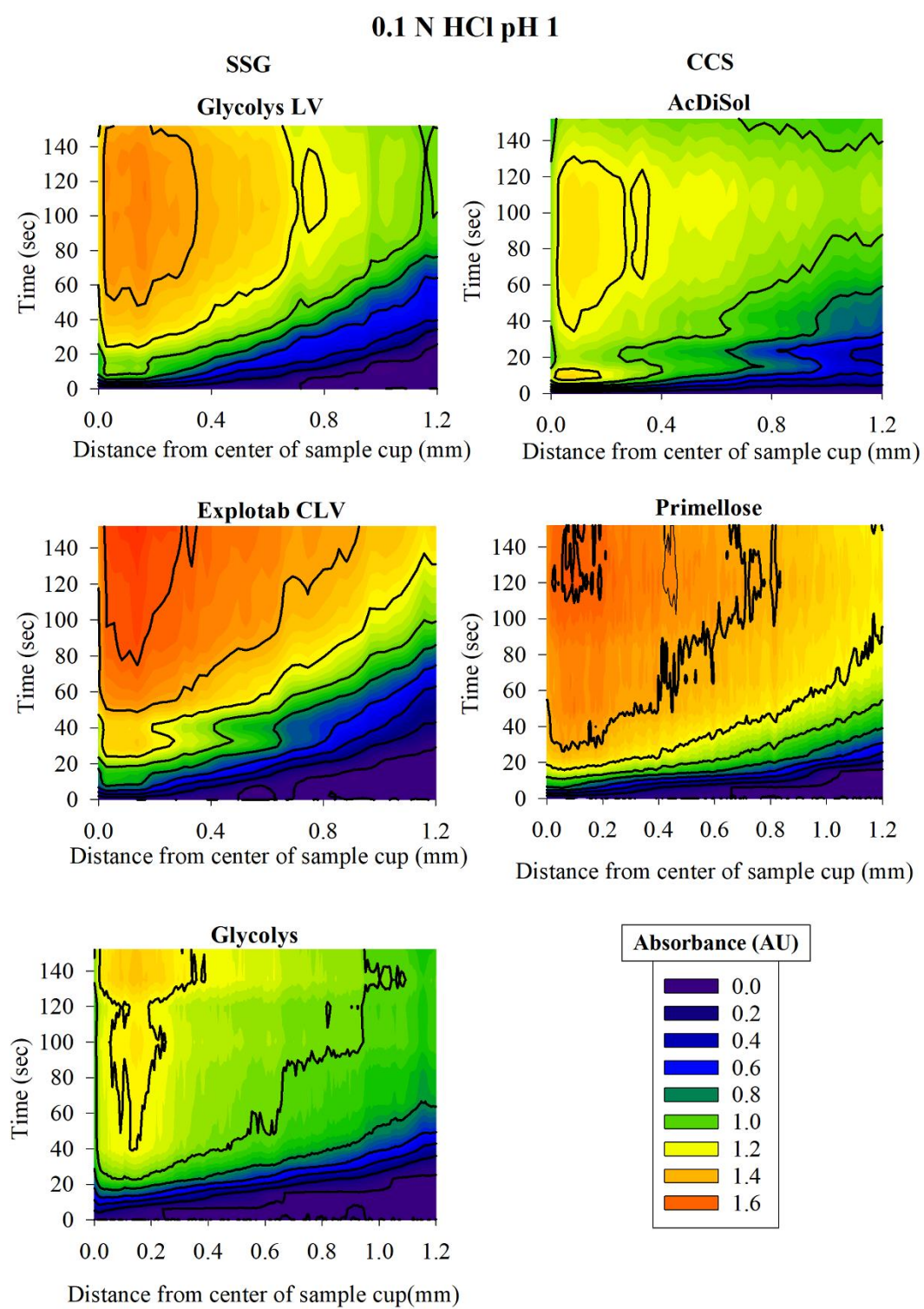
654 studied SSG brands (Glycolys LV: green squares/colour, Explotab CLV: blue
655 diamonds/colour, Glycolys: red triangles/colour). (Mean \pm SD, n =3)

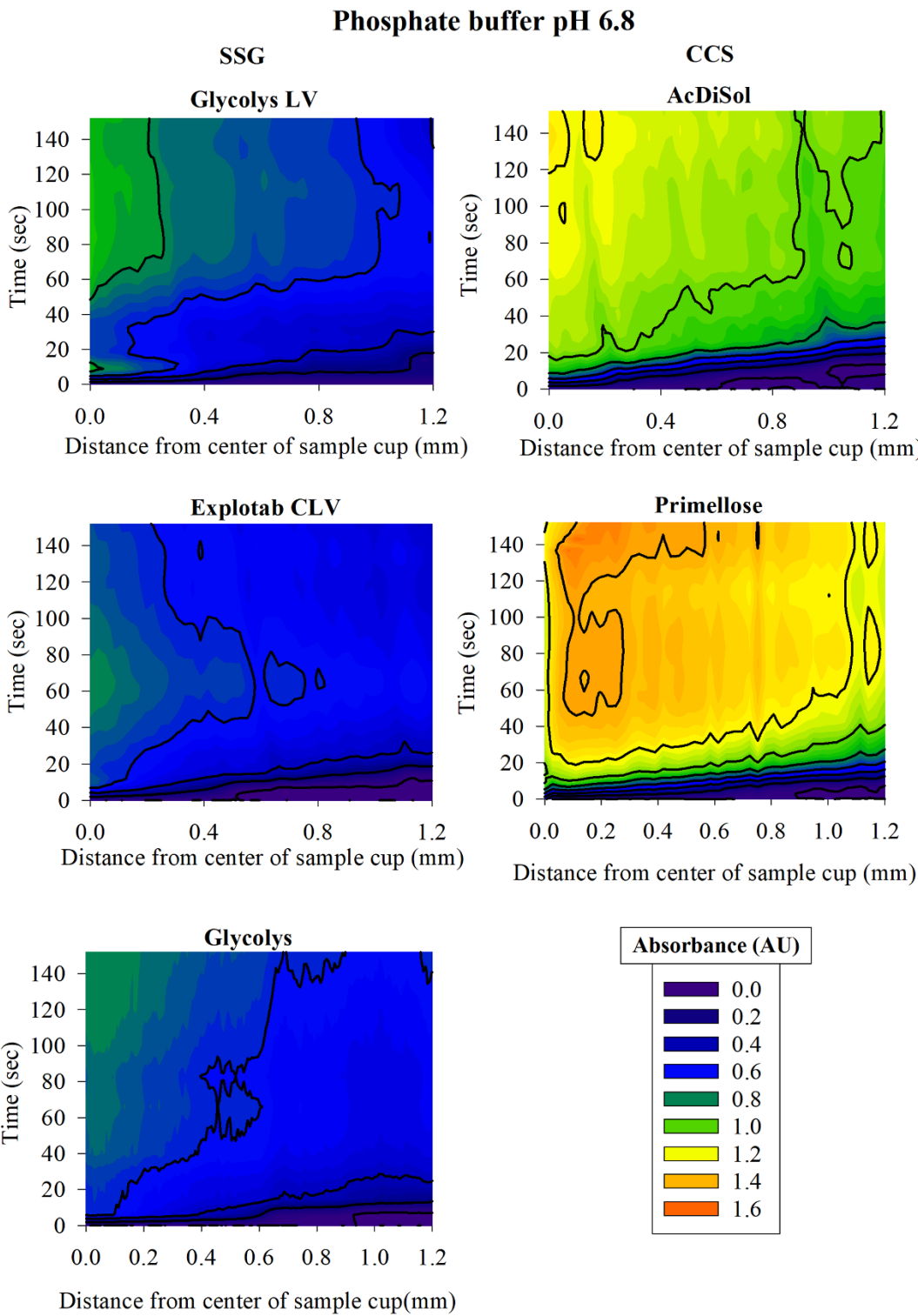
656 **Figure 7:** Cumulative % dissolved (top) and dissolution rates (bottom) of PRC from compacts
657 in a. 0.1 N HCl pH 1 and b. phosphate buffer pH 6.8 using real-time surface dissolution UV
658 imaging (SDi1, 1 mL/min, 37°C) in absence (control: black circles/colour) and presence of the
659 studied CCS brands (AcDiSol: blue squares/colour, Primellose: red diamonds/colour). (Mean
660 \pm SD, n =3)

661 **Figure 8:** Cumulative % dissolved (top) and dissolution rates (bottom) of CBZ from compacts
662 in a. 0.1 N HCl pH 1 and b. phosphate buffer pH 6.8 using real-time surface dissolution UV
663 imaging (1 mL/min, 37°C) in absence (control: black circles/colour) and presence of the
664 studied CCS brands (AcDiSol: blue squares/colour, Primellose: red diamonds/colour). (Mean
665 \pm SD, n =3)

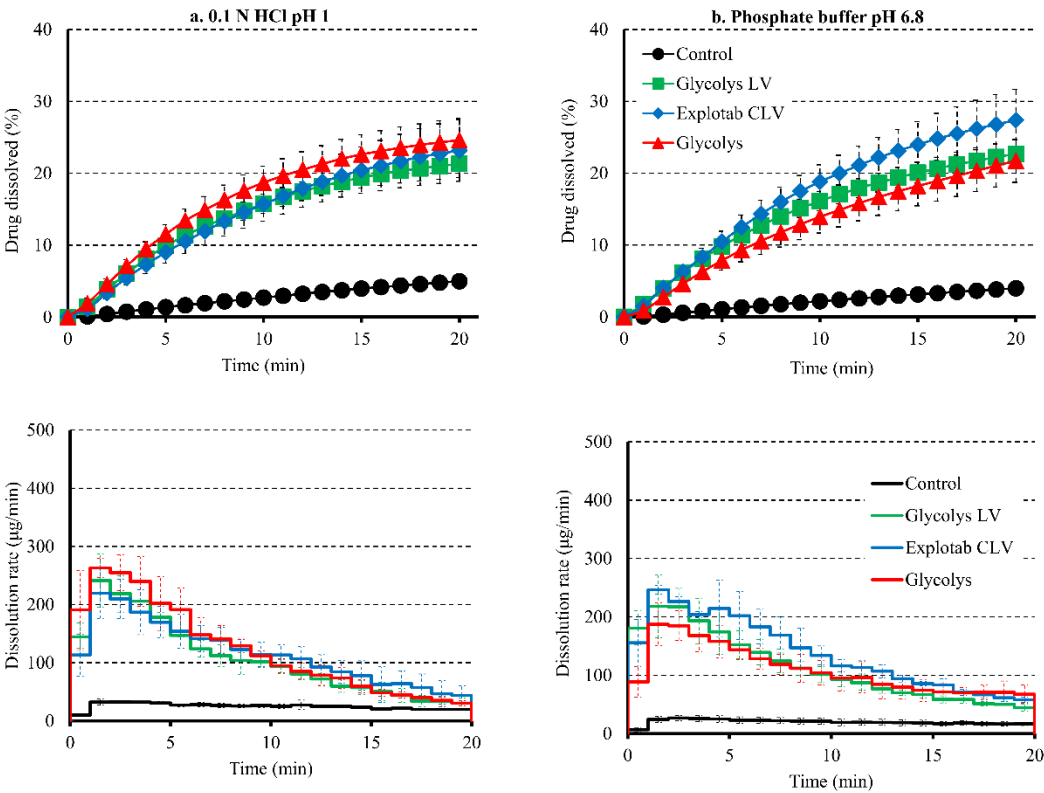
666 **Figure 9:** Standardized coefficients corresponding to the studied variables (and their
667 interactions) for SSG (blue colour) and CCS (red colour). * denotes coefficients with $p < 0.05$.
668 (Mean, - SE) [Exc. Brand: viscosity type for SSG, particle size for CCS].



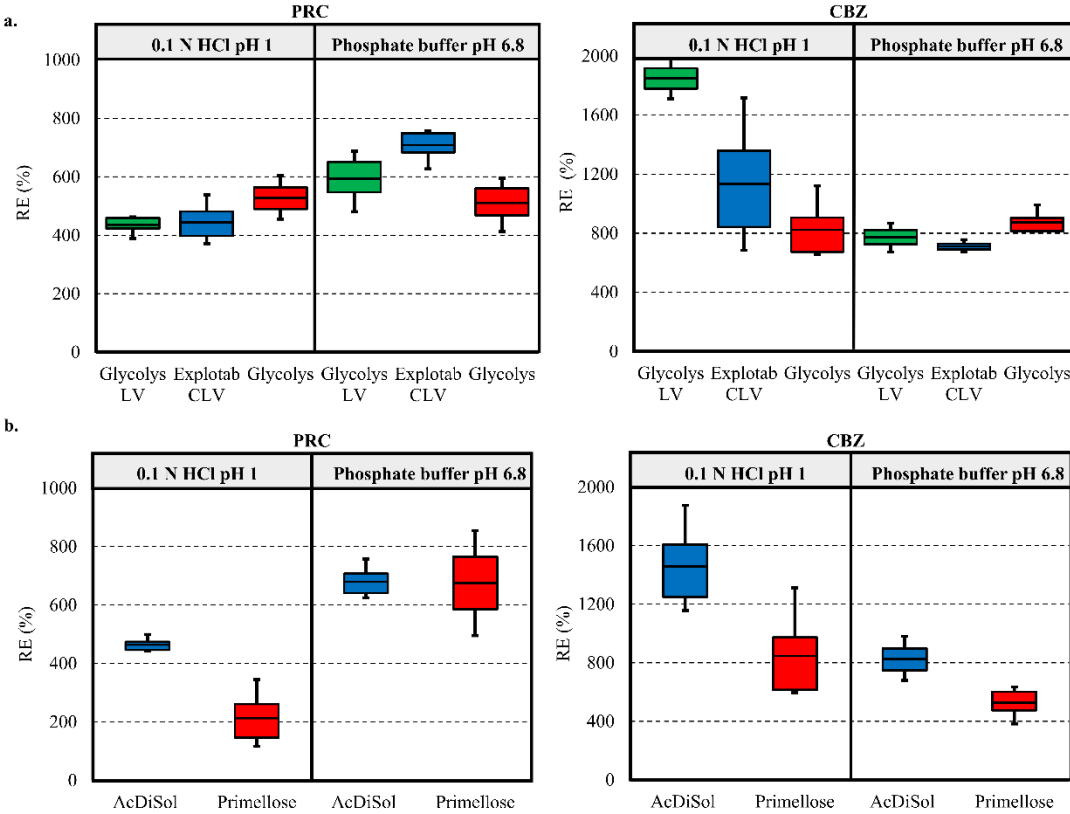


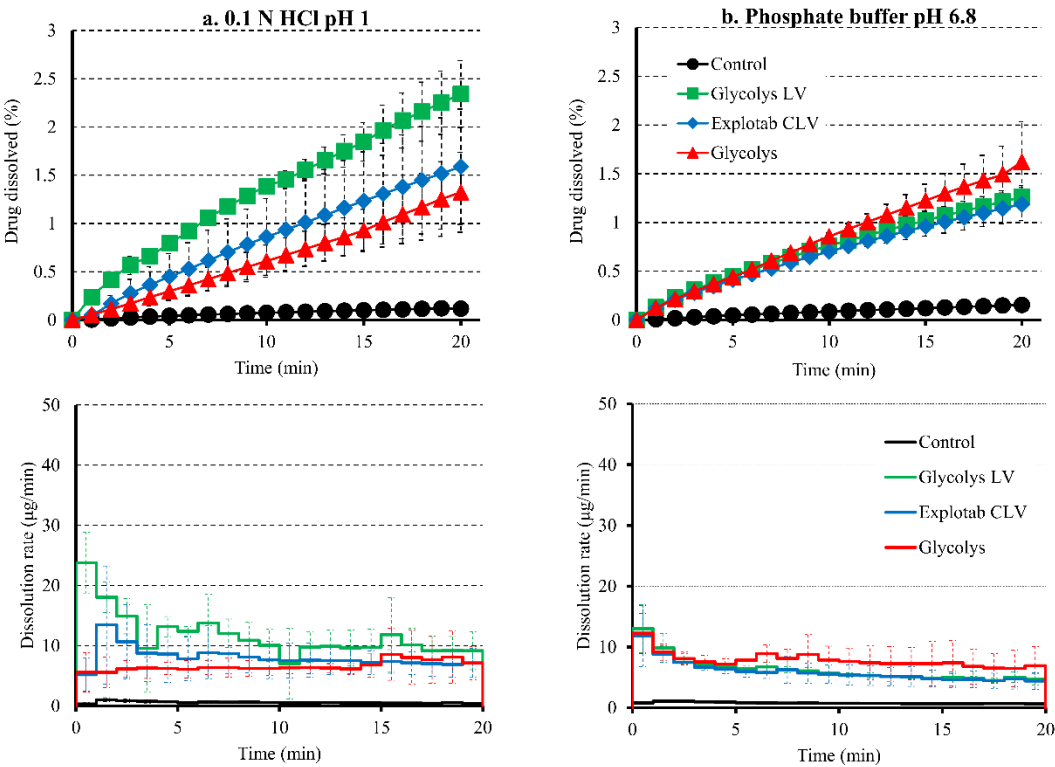


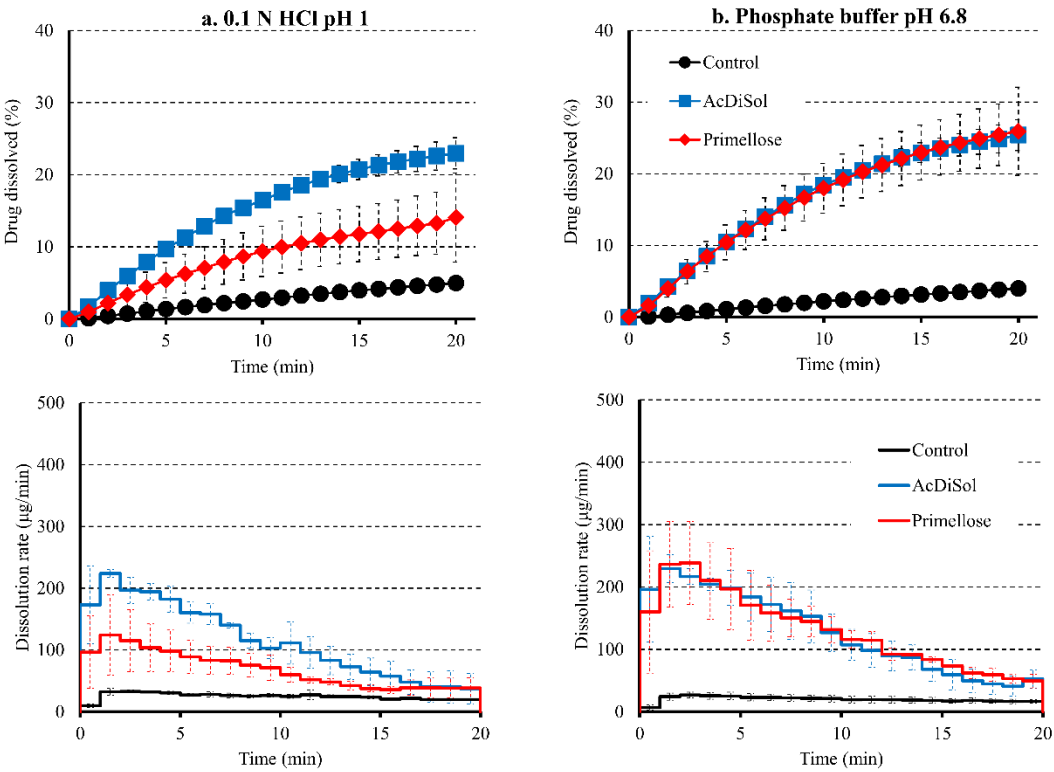
675 **Figure 4**

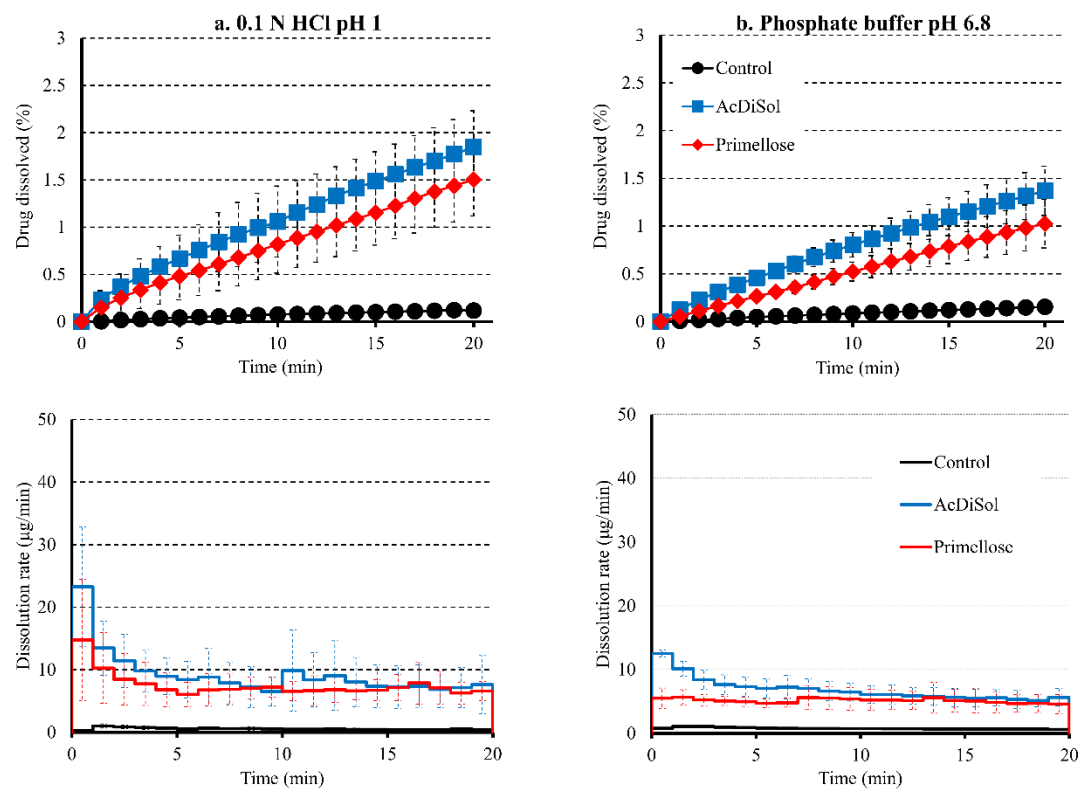


676

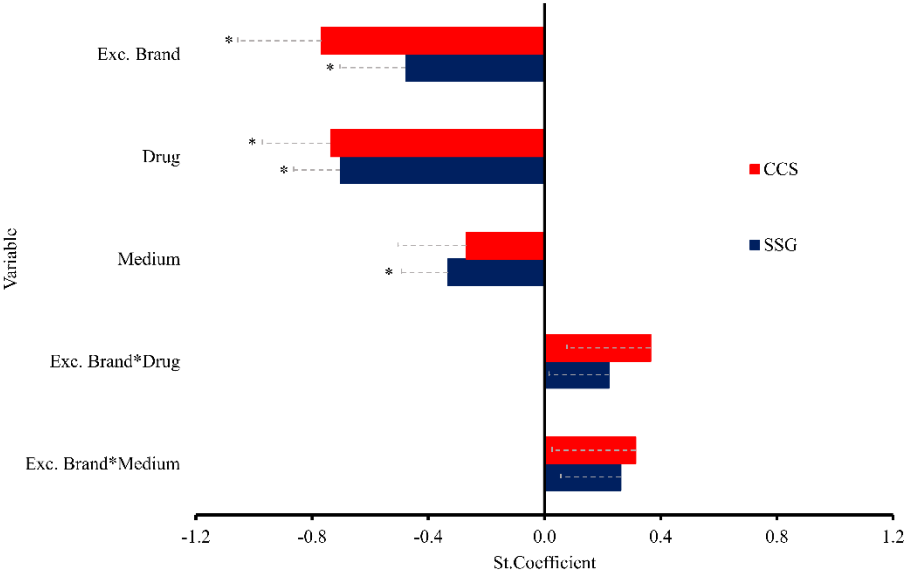








685 **Figure 9**



686